# Comparison of Plastic Instability Analysis and Results of a Vessel Burst Test

## Wolf Reinhardt[1]

[1]Candu Energy / SNC Lavalin, Mississauga, Canada

## ABSTRACT

The burst pressures of two vessels that were pressurized to failure were reported in WRC Bulletin 414 (1996). Failure was observed in the cylindrical potion of the vessel. Analytical expressions for the pressure at plastic instability in a cylindrical shell were obtained for the material stress-strain curve. A comparison based on the Ramberg-Osgood representation showed remarkably good agreement with the experimental burst pressure, given the simple analytical form. A comparison to and discussion of results of a finite element analysis are also included. These results are part of an effort to collect different aspects of technical basis for the application of plastic instability load in the analysis of pressure vessels and piping in service at nuclear plants.

## INTRODUCTION

The present paper discusses a plastic analysis technique mainly in the context of design by analysis of nuclear pressure components using the ASME Code [1] and related fitness-for-service evaluations using specialized guidelines.

When pressurized components are subjected to excessive loading the highest load when failure occurs is typically controlled by one of two mechanisms. If the deformability of the material is limited, fast fracture may occur at the maximum load. With more deformable materials the component reaches a maximum load capacity when work hardening of the material gets balanced by destabilizing changes in geometry of the load bearing wall sections. That the highest load is controlled by plastic deformation effects does not necessarily mean that the subsequent failure (breach of pressure boundary) might not involve some elements of fracture. For example, in a typical tension test of pressure vessel steel, the ultimate strength is due to a plastic mechanism, but the subsequent failure is by fracture, for example by the well known "cup and cone" fracture that combines a shear fracture at the periphery with an overload failure due to internal voiding and rupture in the middle of the specimen. The term "ultimate load" is commonly used to denote the highest load that can be applied before failure occurs.

The prediction of ultimate load is possible based on a suitable plastic analysis methodology [2]. The evaluation of the result then follows the applicable evaluation Code. In Section III of the ASME Boiler and Pressure Vessel Code, plastic analysis has several applications that use different definitions for the allowable load. Section III Subsection NB [1] references the design-by-analysis rules in Appendix XIII, which contains a definition of plastic analysis, namely

***XIII-1300 (u) Plastic Analysis****. Plastic analysis is that method which computes the structural behavior under given loads considering the plasticity characteristics of the materials, including strain hardening and the stress redistribution occurring in the structure.*

The ultimate load is called plastic instability load in Section III. The definition given is

***XIII-1300(w) Plastic Instability Load****. The plastic instability load for members under predominantly tensile or compressive loading is defined as that load at which unbounded plastic deformation can occur without an increase in load. At the plastic tensile instability load, the true stress in the material increases faster than strain hardening can accommodate.*

Although this definition is contained in the general design-by-analysis rules of Appendix XIII, the only place where it is used is mandatory Appendix XXVII [1] of Section III for the purpose of Level D analysis of components in the context of plastic system analysis. Components, which would include piping, may be evaluated according to XXVII-3330using the plastic instability load determined by plastic analysis or experimental analysis. The applied load is limited to 70% of the plastic instability load.

For non-nuclear pressure vessels, the Section VIII Div. 2 [3] rewrite after 2004 introduced a design method based on "plastic collapse load", which is the same as what is called plastic instability load in Section III, and also the same as ultimate load. Although there were efforts to introduce design based on ultimate load into Section III of the ASME Code [1], to date the Section III Code committees have rejected this approach.

On the other hand, a plastic collapse load based approach can be very well suited to address geometrically complicated degradation, such as limited wall loss because the methodology does not rely on somewhat subjective evaluation procedures like stress classification. The plastic collapse load evaluation requires only the load and initial geometry to be known. The evaluation consists of comparing the specified operational load (or load combination) with the plastic instability load obtained by analysis, and ensuring that the latter is higher than the former by the required factor. Such an approach is used in fitness-for-service evaluation procedures, for example ASME FFS-1 [4] and in more specialized industry fitness-for-service guidelines, such as an option in the evaluation of thinned feeder pipes in CANDU reactors as described in [5].

Benchmarking the results of plastic instability analysis against experimental results is important to increase confidence in the method and identify potential areas that need special attention. Such results have been published on a number of different applications, for example for wall thinning in Carbon steel pipes [6], for tubes containing flaws [7], and in comparison to burst disk tests involving significant changes in geometry due to plastic deformation [8], [9]. The implications on using these methods for design were discussed in [9] and [10].

The paper discusses a comparison between the plastic instability pressure obtained from an analytical formula for a cylindrical shell and the results of two burst tests that were published in the literature. The analytical formula includes the effect of plastic strain hardening. Close agreement is achieved. A comparison with the results of a finite element (FE) analysis are also included and discussed.

**TESTS**

Tests of two vessels by pressurization to failure were reported in WRC Bulletin 414 (1996) by Kalnins and Rana [11]. The vessels were cylindrical with an ASME 2:1 elliptical head at one end and a torispherical head on the other end. Testing the torispherical head was the actual main motivation of the experiment, The heads were formed from plate and welded on. The shell had a longitudinal weld seam. The material of shell and heads was carbon steel plate (SA-516 Gr. 70). The vessels were thin-walled with a D/t ratio of about 200, fabricated according to ASME Section VIII Div. 1 requirements.

The primary objective of the test was to evaluate the conservatism of the 1992 version of ASME Section VIII Div. 1 and Div. 2 design rules for torispherical heads. The report [11] provides detailed data on the geometry of the vessel as well as on tensile tests performed on the material. The vessels were instrumented with strain gauges and were pressurized in steps to failure. Figure 1shows the first vessel after completion of the test. The measured shell dimensions are given in Table 1, which also lists the measured tensile properties.

**Table 1: Dimensions of Tested PVRC Vessels [11]**

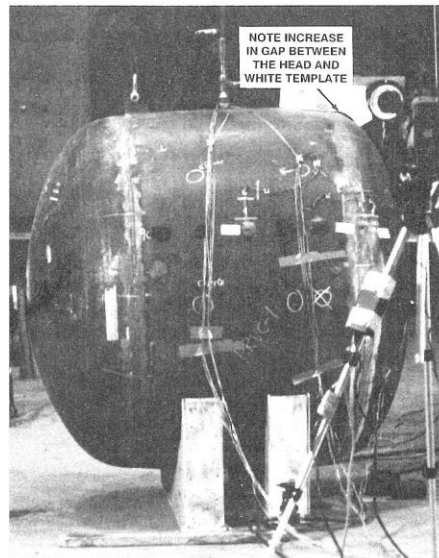|  | **Vessel 1** | **Vessel 2** |
|---|---|---|
| Cylindrical Shell Mean Radius, $r_m$ | 30.16 in | 30.20 in |
| Cylindrical Shell Thickness (meas.), $t$ | 0.269 in | 0.314 in |
| Cylindrical Shell $t/r_m$ | 0.00892 | 0.0104 |
| Cylindrical Shell Length | 36 in | 36 in |
| Elliptical Head Type | ASME 2:1 | ASME 2:1 |
| Elliptical Head Thickness (nom) | 0.31in | 0.31 in |
| Torispherical H. Knuckle Radius (meas.) | 3.75 in | 3.75 in |
| Torispherical H. Crown Ins. Radius | 59 in | 59.5 in |
| Torispherical Head Thickness (meas.) | 0.25 in | 0.32 in |
| Shell and Head Material | SA-516 Gr. 70 | SA-516 Gr. 70 |
| Measured Yield Strength, $\sigma_y$ | 52.9 ksi | 56.6 ksi |
| Measured Ultimate Tensile Strength, $\sigma_u$ | 77.5 ksi | 84.4 ksi |
| Measured Uniform Elongation, $\varepsilon_u$ | 19.1% | 17.8% |



**Figure 1: PVRC Test Vessel 1 after Pressurization(from PVRC Bulletin 414[11])**

After the conclusion of each test, when failure had occurred, metallurgical examinations were performed to determine the failure mode and the originating site for the failure. Vessel 1 was determined to have suffered a brittle through-wall failure (leak) originating from one of the nozzles with lack of fusion in one of the attachment welds. The failure of the second vessel originated at the long seam of the cylindrical shell and resulted in a gross failure of the entire shell. The failure of Vessel 2 was considered ductile. Neither vessel failed in the heads.

## THEORETICAL BACKGROUND

Based on the work of Considère [12], the point of tensile instability for plastic deformation can be derived from the condition that the increment of force sustained by a portion of the wall becomes zero. For a cylinder with closed ends under an applied pressure $p$, the hoop stress is the maximum tensile principal stress $\sigma_h = \sigma_1$ and is related to the internal pressure, $p$, by

$$p = \frac{t}{r_m}\sigma_1 \tag{1}$$

where $t$ and $r_m$ are the deformed thickness and mean radius of the shell, respectively. The condition of plastic instability allowing no increment in load, $dp=0$, then results in

$$d\sigma_1 = \sigma_1 \left(\frac{dr_m}{r_m} - \frac{dt}{t}\right). \tag{2}$$

Using the principal true plastic strain, $\varepsilon_1 = dr_m/r_m$ and the condition that plastic deformation leaves the volume constant, the structural instability condition becomes

$$\frac{d\sigma_1}{d\varepsilon_1} = 2\sigma_1 \tag{3}$$

Let the true stress-strain curve be described with a power law (Ramberg-Osgood material)

$$\sigma_t = C_{RO}\varepsilon_{tp}{}^n \tag{4}$$

Where $\sigma_t$ is the equivalent true stress, $\varepsilon_{tp}$ is the equivalent true plastic strain, $n$ is the strain hardening exponent and $C_{RO}$ is the Ramberg-Osgood modulus. Relating the equivalent stress and strain at the point when Equation (3) is satisfied to the largest tensile principal stress and strain, the equivalent true stress at the ultimate pressure can now be calculated as

$$\sigma_{t,\ eq} = C_{RO}\varepsilon_{t,\ eq}{}^n = C_{RO} \left(\frac{\sqrt{3}}{3}\right)^n n^n \tag{5}$$

Since $(\sqrt{3}/3)^n$ is less than unity, the equivalent wall stress in the cylinder at the point of instability will be less than the true ultimate stress, i.e. the instability point is predicted to occur at a lower stress than in a tension test. For a moderately thin shell, the first-order accurate expression for calculating the average true hoop stress is

$$\sigma_{t,\ h} = \frac{2\sqrt{3}}{3}\frac{\sigma_{t,\ eq}}{1+\frac{1}{2}\frac{t}{r_m}} = \frac{2C_{RO}}{1+\frac{1}{2}\frac{t}{r_m}}\left(\frac{\sqrt{3}}{3}\right)^{n+1} n^n \tag{6}$$

The ultimate pressure is then

$$p_{u,RO} = 2C_{RO}\left(\frac{\sqrt{3}}{3}\right)^{n+1}\frac{1}{1-\frac{1}{4}\left(\frac{t_0}{r_{m0}}\right)^2 e^{-2n}}\frac{t_0}{r_{m0}}\left(\frac{n}{e}\right)^n \tag{7}$$

where $t_0$ and $r_{m0}$ are the initial shell thickness and mean radius, respectively. The ultimate strength, $\sigma_u$, from a tensile test is given by

$$\sigma_u = C_{RO} \left(\frac{n}{e}\right)^n \tag{8}$$

and thus, Equation (7) can be expressed as

$$p_{u,RO} = 2\left(\frac{\sqrt{3}}{3}\right)^{n+1} \left[\frac{1}{1-\frac{1}{4}\left(\frac{t_0}{r_{m0}}\right)^2 e^{-2n}}\right] \frac{t_0}{r_{m0}} \sigma_u. \tag{9}$$

Neglecting the second-order term in the thickness ratio in the denominator of Equation (9), the relationship between the ultimate pressure, $p_{u,Cyl}$, and the ultimate tensile strength, $\sigma_u$, of the same material, Equation (8), becomes

$$p_{u,cyl} \approx 2 \left(\frac{\sqrt{3}}{3}\right)^{n+1} \frac{t_0}{r_{m0}} \sigma_u. \tag{10}$$

This expression was given by Gerdeen [13] and Rodabaugh [14] based on a derivation by Cooper [15]. Rodabaugh noted in [14], that Equation (10) and similar ones " *have sound theoretical foundations and check well with burst test data on pipe.*".

For piping and pressure vessel carbon steels, the value of *n* is about 0.15 to 0.2, and the factor $2(\sqrt{3}/3)^{n+1}$ is between 1.03 and 1.07, or close to unity. This is consistent with Rodabaugh's observation [14] that "*… the following much simpler equation also checks well with burst test data on pipe...*"

$$p_{u,simp} = \frac{t_0}{r_{m0}} \sigma_u \tag{11}$$

Using a similar derivation as that to arrive at Equation (10), an expression for the ultimate pressure of a sphere, $p_{u,sph}$, can be obtained giving

$$p_{u,sph} \approx 2\left(\frac{1}{3}\right)^n \frac{t_0}{r_{m0}} \sigma_u. \tag{12}$$

Equation (10) and (12) are used to calculate analytical estimates of the ultimate pressure.

**ANALYSIS**

The formula for the plastic collapse load of a cylinder, Equation (10), was used to calculate the burst pressures for the two vessels based on plastic instability using the measured dimensions and tensile properties. The true stress-strain curve was assumed to be described by a power law with hardening exponents *n* = 0.175 for Vessel 1 and *n* = 0.164 for Vessel 2, as derived from the uniform tensile elongations of tensile tests of the plate material used for the vessels.

For comparison, a finite element (FE) analysis of the entire vessel shell was performed. The model and boundary conditions are shown in Figure 2. The model is created from axisymmetric shell elements that are capable of implementing nonlinear material and a large deformation / large strain formulation (the left picture in Figure 2 shows a view that is expanded to a full 360°). A quarter model meshed with 8-noded quadrilateral shell elements was also analyzed. On the right, Figure 2 shows that internal pressure is applied to all surfaces, and that displacement boundary conditions are used to prevent rigid body motions but not otherwise restrict the deformation in any way. The analysis uses large deformation options and is based on true stress and true strain. The plastic instability load is determined as that load where the FE software cannot establish equilibrium under a further increase in load. In practice, that means that the implicit FE solver fails to converge beyond the plastic instability load.

Elastic-plastic analysis based on a representation of the measured stress-strain curves from tensile tests is performed. For this purpose measured engineering stress-strain curves given in [11] were digitized and converted into true stress – true strain curves (shown below in the results Section of this paper). Two material models that are available in the FE software (ANSYS 19.0), multilinear isotropic hardening and

power law isotropic hardening are compared. Multilinear isotropic hardening is used to implement a close approximation of the measured stress-strain curves, while is power law isotropic hardening a fit to the measured curve is performed.



**Figure 2: Finite Element Model and Boundary Conditions**

**RESULTS AND DISCUSSION**

*Comparison of Experimental Ultimate Pressure and Prediction Based on Failure Mechanism*

The experimental outcomes indicated that in both cases failure occurred in the cylindrical portion of the vessel. To compare the experimental ultimate pressure with the appropriate analytical result, it was therefore decided to use Equation (10) for a cylinder. The analytical and experimental ultimate (failure) pressures in Table 2 show that the two are in good agreement. The results are within 15% of each other. Test vessel 1 failed slightly below the predicted failure pressure of the cylinder. However, this failure occurred at a flaw in the nozzle weld and was only local (leak) which means that the failure pressure of the entire vessel was not reached at this point. Test vessel 2 failed at a higher pressure than predicted based on a cylindrical geometry. This indicates that there could be an effect of the attached heads on ultimate pressure.

**Table 2: Plastic Instability Loads of PVRC Vessels and Analytical Result for Cylinder**

| Plastic Instability Load | | Vessel 1 | Vessel 2 |
|---|---|---|---|
| Ultimate Pressure | Experimental WRC 414 (1996) | 700 psi | 1080 psi |
| | Analytical Cylinder (10) | 719 psi | 923 psi |

In elastic analysis, a decay length of $2.5\sqrt{r_m t}$, is used for cylindrical shells, where $r_m$ is the mean radius and $t$ is the thickness. The decay length describes how far from the edge (global discontinuity) of a shell axisymmetric edge effects have decayed to a small disturbance of the stress distribution in the shell. For the present cylindrical shell, the elastic decay length is about 8 in. Since the cylindrical shell is 36 in long, one would expect that the middle 20 in of it would be undisturbed by effects from the heads. Whether this expectation is verified for the large deformation plastic state of the shell near the plastic instability load is investigated by performing a finite element analysis of the vessels.

*Comparison of Experimental Ultimate Pressure and FE Vessel Simulation*

The ultimate pressure for the two test vessels is compared with the result of FE analysis in Table 3. The ultimate pressure obtained from FE is seen to be significantly higher than that from the tests. A review of the deformed shape of the vessel showed that near the point of plastic instability the vessel had deformed into a practically spherical shape. Failure in analysis did, therefore, not occur with cylindrical geometry but rather in a nearly spherical shape. Evidently, elastic decay length does not apply to the present large deformation plastic condition. The transition to a sphere represents a case of geometric strengthening, i.e., the sphere has a higher ultimate pressure than the cylinder. It is also noted that the total surface area of the vessel is close to that of a sphere with 30 in radius. This will be explored further later in this Section.

**Table 3: Plastic Instability Loads of PVRC Vessels Compared with FE Result**

| Plastic Instability Load | | Vessel 1 | Vessel 2 |
|---|---|---|---|
| Ultimate Pressure | Experimental WRC 414 (1996) | 700 psi | 1080 psi |
| | FE, Vessel Model | 1128 psi | 1417 psi |

Since the test vessels failed at a lower pressure than the plastic instability load, it is concluded that both vessels failed by exhaustion of ductility rather than plastic instability. Section VIII Div. 2 gives a limit on the equivalent At the pressures shown in Table 2 the shape of the vessel is still close to cylindrical. This is consistent with the post-test image (Figure 1).
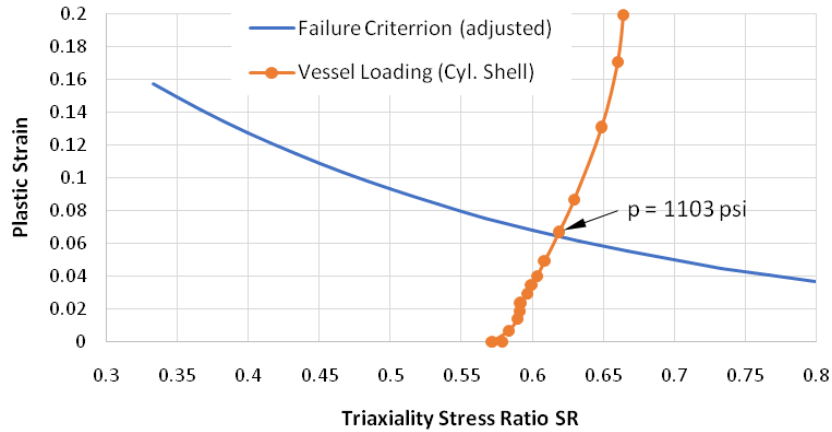


**Figure 3: Equivalent Plastic Strain in Shell of Vessel 2 FE Model and Failure Line**

Section VIII Div. 2, Part 5 [3] has a strain based failure criterion for the equivalent plastic strain, $\varepsilon_{p,eq}$, of the general form

$$\varepsilon_{p,eq} \leq \varepsilon_{Lu} e^{-\frac{\alpha_{SL}}{1+m_2}\left(SR-\frac{1}{3}\right)} \tag{13}$$

where SR is the triaxiality stress ratio, i.e. the ratio of average hydrostatic stress to von Mises equivalent stress. $\varepsilon_{Lu}$ is the uniaxial failure strain from a tensile test, determined by the rules of Part 5, $\alpha_{SL}$ is a material dependent constant and $m_2$ is calculated from the ratio of room temperature yield to ultimate strength, again material dependent as specified by the rules of Part 5 of [3]. The evaluation was performed following Part 5, but the calculated strain limit did not lower the failure pressure significantly.

In Figure 3, the equivalent plastic strain obtained from a location near the midpoint of the cylindrical shell of Vessel 2 is plotted against the triaxiality stress ratio, SR, at the same location. Only Vessel 2 is shown

because the failure of Vessel 1 was governed by a flaw. It can be seen that at low load and deformation, SR has the value expected for a thin cylinder, $\sqrt{3}/3 \approx 0.577$. As the load and deformation increases, the triaxiality stress ratio approaches the value for a thin sphere, $2/3 \approx 0.667$.

For illustration, the failure criterion is also shown. Equation (13) was adjusted with constants different from those in [3] for ferritic material, namely $\alpha_{SL} = 4$, indication greater sensitivity to multiaxial stress states, and $\varepsilon_{Lu} = 0.17$, i.e. lower strain at failure. The resulting failure curve would indicate failure just below 1103 psi, versus an experimental failure pressure of 1080 psi. Since failure in the test of Vessel 2 occurred in the longitudinal seam of the cylindrical shell, it is quite possible that the cause was lower ductility of the weld material relative to base material. This may explain that the constants for Equation (13) had to be adjusted and a possible higher sensitivity to the triaxial stress ratio.

Since the nozzles are adequately reinforced and, if properly welded (unlike Vessel 1), are not expected to affect the failure pressure, it is expected that the present model adequately represents the failure mechanism and including the nozzles in the model is not necessary.

### *Effect of Stress-Strain Curve Modelling in FE Simulation*

To investigate the effect of the material description used in the FE analysis, two models were compared. One was the multilinear description of the measured stress-strain curve (converted to true stress-strain) and the other a power law description similar to Equation (4), Figure 4. Although the two curves differed particularly near the onset of yielding, the burst pressures were almost identical. This confirms that good agreement is achieved with the Power Law representation by matching the ultimate strength (Equation (8)) and the approximate shape of the stress-strain curve at higher strains.

**Table 4: FE Plastic Instability Loads for Different Material Models**

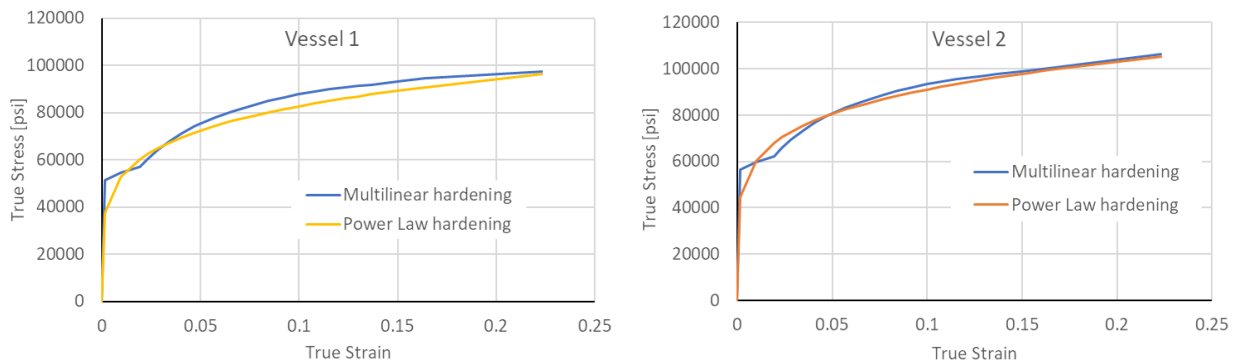| Plastic Instability Load | | Vessel 1 | Vessel 2 |
|---|---|---|---|
| Ultimate Pressure | FE, Vessel Model, Multilinear | 1128 psi | 1455 psi |
| | FE, Vessel Model, Power Law | 1111 psi | 1417 psi |



**Figure 4: Comparison of True Stress – True Strain Curves for FE Material Models**

When using the multilinear representation, it was found to be important that the stress-strain curve is discretized finely enough in the region of interest. In the present case, 20 stress-strain points were used along the curve.

### *Effect of Vessel Length in FE Simulation*

The elastic-plastic analysis for the present vessel predicted a failure pressure above that of a simple cylindrical vessel. This is attributed to the constraint from the heads, and one should logically expect that

a vessel with a long enough cylindrical shell would have the ultimate pressure of a cylindrical shell. The results in Table 5 show that this is the case. The ultimate pressure of the present vessel with the cylindrical shell elongated to 180 in obtained by FE analysis agrees almost perfectly with that from the cylindrical shell Equation (10). It is also shown that the actual vessel with a 36 in shell has a failure pressure very close to that of a spherical shell with 30 in radius as suggested by the relatively close agreement is surface area between the present vessel and such a sphere that was mentioned earlier.

**Table 5: Plastic Instability Analytical and FE Results**

| Plastic Instability Load | | Vessel 1 | Vessel 2 |
|---|---|---|---|
| Ultimate Pressure | FE, Vessel Model | 1128 psi | 1417 psi |
| | Analytical, Sphere, eq. (12) | 1119 psi | 1450 psi |
| | FE, Elongated Vessel Model | 718 psi | 926 psi |
| | Analytical, Cylinder , eq.(10) | 719 psi | 923 psi |

A variation of the shell length resulted in the change in ultimate pressure indicated in Figure 5. The ultimate pressure of a cylinder is approached closely with a shell length of about 70 in. This corresponds to a shell length from each of the shell/head discontinuities of about 1 to 1.5 times the shell radius, which one could call the decay length of the present elastic-plastic solution. This is very significantly longer than the decay length known from elastic shells.
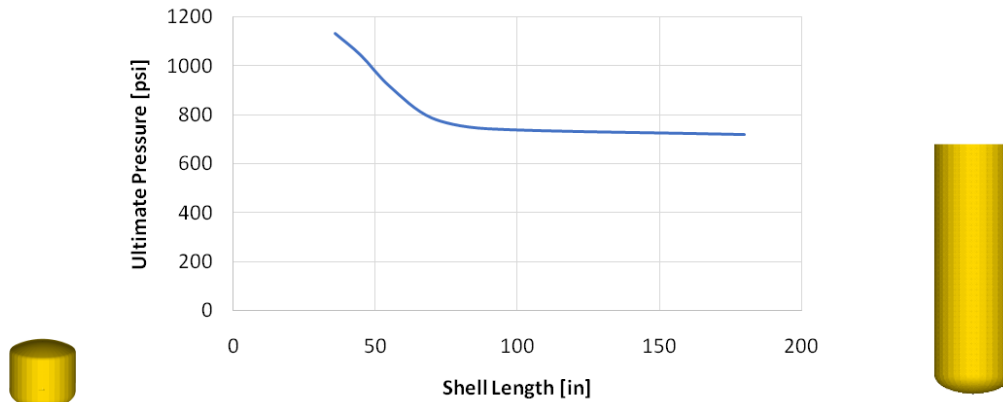


**Figure 5: Effect of Shell Length on Ultimate Pressure**

**CONCLUSION**

The burst pressures of two vessels that were pressurized to failure were reported in WRC Bulletin 414 (1996). Failure was observed in the cylindrical potion of the vessel. Analytical expressions for the pressure at plastic instability in a cylindrical shell were obtained for various representations of the material stress-strain curve. A comparison based on the Ramberg-Osgood representation showed remarkably good agreement with the experimental burst pressure, given the simple analytical form.

Finite element analysis of the vessels showed that the predicted ultimate pressure is higher than that of the cylindrical shell. The reason was determined to be that the deformation of the cylindrical shell is influenced by the constraint exerted by the heads. It was also determined that the failure of the tested vessels was determined by the onset of ductile rupture rather than pure plastic collapse. It is likely that reduced ductility in the region of the longitudinal weld was the cause of failure, since the criterion for "local failure" from Section VIII Div. 2 indicated a higher rupture strain for base material.

This result is part of an effort to collect different aspects of technical basis for the application of plastic instability load in the analysis of pressure vessels.

**REFERENCES**

[1]     ASME Boiler and Pressure Vessel Code (2021), Section III, *Rules for Construction of Nuclear Facility Components,* ASME, New York.

[2]     Updike, D.P., and Kalnins, A., *Ultimate Load Analysis for Design of Pressure Vessels*, PVP Vol. 353, Pressure Vessel and Piping Codes and Standards, ASME Pressure Vessel and Piping Division Conference, 1997.

[3]     ASME Boiler and Pressure Vessel Code (2021), Section VIII, *Rules for Construction of Pressure Vessels*, Division 2, *Alternative Rules,* ASME, New York.

[4]     ASME FFS-1 (2021), *Fitness-for-Service*, ASME, New York.

[5]     Duan, X., Kozluk, M.J., & Li, M. (2009), *Comprehensive Integrity Assessment of Carbon Steel Feeder Pipes/Elbows Subject to Wall Thinning*. Proceedings of the ASME 2009 Pressure Vessels and Piping Conference. Volume 6: Materials and Fabrication. Prague, Czech Republic. July 26–30, 2009. pp. 847-858.

[6]     Reinhardt, W, & Duan, X. "Comparison of Elastic-Plastic Analysis and Experimental Result for Locally Thinned Pipe." Proceedings of the ASME 2010 Pressure Vessels and Piping Division/K-PVP Conference. ASME 2010 Pressure Vessels and Piping Conference: Volume 3. Bellevue, Washington, USA. July 18–22, 2010. pp. 279-286.

[7]     Kyu,  I. S., and Park, J.-H. (2007), *Analysis of Burst Pressure of Damaged Tubes Using Plastic Instability Analysis*, Solid State Phenomena Vol. 120, pp. 187-192.

[8]     D. P. Jones, J. E. Holliday (2000), *Elastic-Plastic Analysis of the PVRC Burst Disk Tests With Comparison to the ASME Code Primary Stress Limits*, ASME J. of Pressure Vessel Technology Vol. 122, pp. 146-151.

[9]     Reinhardt, W. (2009), *Investigation of the Elastic-Plastic Design Method in Section VIII Div. 2*. Proceedings of the ASME 2009 Pressure Vessels and Piping Conference. Volume 1: Codes and Standards. Prague, Czech Republic. July 26–30, 2009. pp. 41-50.

[10]   Carmichael, R, & Mackenzie, D.(2010), *Elastic-Plastic Design by Analysis for Gross Plastic Collapse.* Proceedings of the ASME 2010 Pressure Vessels and Piping Division/K-PVP Conference. ASME 2010 Pressure Vessels and Piping Conference: Volume 2. Bellevue, Washington, USA. July 18–22, 2010. pp. 81-87.

[11]   Kalnins, A., and Rana, M.D. (1996), *A New Design Criterion Based on Pressure Testing of Torispherical Heads*, WRC Bulletin414, Welding Research Council, Inc., New York.

[12]   Considère, A. (1885), *Mémoire sur l'emploi du fer et de l'acier dans les constructions*, Annales des Ponts et Chaussées, 9, pp. 574-775.

[13]   Gerdeen, J.C., *A Critical Evaluation of Plastic Behaviour Data and A United Definition of Plastic Loads for Pressure Components*, WRC Bulletin 254, November 1979.

[14]   Rodabaugh, E.C., *Interpretive Report on Limit Analysis and Plastic Behavior of Piping Products*, WRC Bulletin 254, November 1979.

[15]   Cooper, W.E., *The Significance of the Tensile Test to Pressure Vessel Design*, Welding Research Supplement, Jan. 1957, p. 49-S.

[16]   Kalnins, A.  and Updike, D. P. (1996) *Analysis of Failure of a Torispherical Head Under Internal Pressure*, ASME PVP Conference, 338, 265–271.